Stability Margin Scaling Laws for Distributed Formation Control as a Function of Network Structure

He Hao, Prabir Barooah, and Prashant G. Mehta

***Abstract*— We describe a methodology for modeling, analysis, and distributed control design of a large vehicular formation whose information graph is a D-dimensional lattice. We derive asymptotic formulae for the closed-loop stability margin based on a PDE approximation of the formation. We show that the exponent in the scaling law for the stability margin is influenced by the structure of the information graph and by the control architecture (symmetric or asymmetric). For a given fixed number of vehicles, we show that the scaling law can be improved significantly by employing a higher dimensional information graph and/or by introducing small asymmetry (mistuning) in the nominally symmetric proportional control gains. We also provide a characterization of the error introduced by the PDE approximation.**

***Index Terms*— Distributed control, formation control, mistuning, partial differential equation, stability margin.**

I. Introduction

We consider the problem of distributed control of a large vehicular formation. The control objective is that vehicles maintain a desired formation geometry while following a constant-velocity type desired trajectory. The desired formation geometry is specified in terms of desired relative positions between pairs of vehicles. The desired trajectory of the formation is specified in terms of trajectories of a few lead vehicles. The problem is relevant to a number of applications such as formation control of aerial, ground, and autonomous vehicles for transportation, surveillance, reconnaissance, mine-sweeping etc. [1], [2].

Each vehicle is modeled as a fully actuated point mass. This means that (i) the dynamics of each coordinate of the vehicle's position are modeled using a double integrator, (ii) the dynamics along the coordinates are decoupled, and (iii) an independent force control input actuates each coordinate. A distributed control law is examined: the control input for an individual vehicle depends on (i) its own velocity and (ii) the relative position measurements with a small subset of vehicles (neighbors) in the formation. The neighbor relationship is defined according to an *information graph*. The existence of an edge (i, j) in the graph means i and j can measure each other's relative position and use that in computing their respective control inputs.

The information graph has been recognized to play an important role in closed-loop stability of the formation [3], [4]. In a recent work, Bamieh *et. al.* studied controlled *symmetric* vehicle formations with a D-dimensional torus as the information graph [5]. Scaling laws, as a function of number of vehicles N, are considered for certain performance measures that quantify the sensitivity of the closed-loop to stochastic disturbance. The scaling laws are shown to depend on the dimension D of the information graph.

The scaling laws of stability margin – defined as the absolute value of the real part of the least stable closed-loop eigenvalue - for one-dimensional platoons, and their dependence of asymmetry in control gains, have been examined previously in [6]. An extension to two-dimensional formations is considered in [7].

In this paper, we investigate scaling laws for stability margin of the closed-loop as a function of i) number of vehicles, ii) structure of the information graph, and iii) the control architecture (symmetric or asymmetric control gains). We limit the study to a special class of information graphs, namely, D-dimensional (finite) lattices. A lattice is a natural choice in formations where relative measurements are available between vehicles that are physically close [8].

The analysis of this paper is based on a PDE approximation of the formation. Such a PDE approximation was originally proposed in [6] for analysis of one-dimensional lattice; such approximations have also been considered in [9] for multi-agent coordination problems. A similar methodology based on partial difference equations has been developed in [10]. In this paper, we extend the one-dimensional analysis of [6] to D-dimensional lattices. We show that for a square lattice with symmetric control architecture, the stability margin scales as $O(1/N^{2/D})$ for large N. Thus, one can improve the stability margin by deploying a higher dimensional information graph. For a non-square information graph, it is possible to improve the stability margin as a function of N. In fact, it is even possible to make the stability margin independent of N. The price one pays for such improvement is either long range communication between vehicles and/or increased number of lead vehicles.

The stability margin can be further improved by introducing small amount of asymmetry (mistuning) in the control gains. In particular, the stability margin for a square information graph with mistuned control gains scales as $O(1/N^{1/D})$ – i.e., the exponent is reduced by a factor of 2 compared to the symmetric case. In the mistuned design, information from distinct neighbors is weighted differently according to an optimal mistuning profile. Certain details that have been omitted due to space limitations appear in a companion paper [11].

II. Problem statement

We consider the formation control of N identical vehicles. The position of each vehicle is a D_s-dimensional vector (with $D_s \geq 1$). D_s is referred to as the *spatial dimension* of the formation. Let $p_i^{(\mathrm{d})} \in \mathbb{R}$ be the d-th coordinate of the i-th vehicle's position, whose dynamics are modeled by a double integrator:

$$\ddot{p}_i^{(\mathrm{d})} = u_i^{(\mathrm{d})}, \quad \mathrm{d} = 1, \ldots, D_s, \tag{1}$$

where $u_i^{(\mathrm{d})} \in \mathbb{R}$ is the control input. The underlying assumption is that the vehicles are *fully actuated*:

Assumption 1: Each of the D_s coordinates of a vehicle's position can be independently actuated. □

The control objective is that the vehicles maintain a desired rigid formation geometry while following a desired trajectory. The desired formation geometry is specified by the desired values of $p_i^{(\mathrm{d})}(t) - p_j^{(\mathrm{d})}(t)$ for *every* pair of vehicles (i, j). The desired inter-vehicular spacing is denoted by $\Delta_{i,j}^{(\mathrm{d})}$ along the d-axis of a Euclidean coordinate system. These spacings must be mutually consistent, i.e., $\Delta_{i,j}^{(\mathrm{d})} = \Delta_{i,k}^{(\mathrm{d})} + \Delta_{k,j}^{(\mathrm{d})}$ for every triple i, j, k. Since we consider rigid formations, $\Delta_{i,j}^{(\mathrm{d})}$'s are assumed to be constant and known a priori.

In this paper, we consider the desired reference trajectory of the formation to be of constant-velocity type and it is known only to a few lead vehicles. We introduce N_r fictitious "reference vehicles", one for each lead vehicle. A reference vehicle perfectly tracks its own desired trajectory, and the lead vehicle can measure the relative position between itself and its corresponding reference vehicle.

The control law is distributed and described in terms of an *information graph*:

Definition 1: An *information graph* is an undirected graph $\mathbf{G} = (\mathbf{V}, \mathbf{E})$, where the set of *nodes* $\mathbf{V} = \{1, 2, \ldots, N, N+1, \ldots, N+N_r\}$ consists of N real vehicles and N_r reference vehicles. Two nodes i and j are called *neighbors* if $(i, j) \in \mathbf{E}$, and the set of neighbors of i are denoted by $\mathcal{N}_i$. □

This work was supported by the National Science Foundation through Grants CNS-0931885 and ECCS-0925534, and by the Institute for Collaborative Biotechnologies through grant DAAD19-03-D-0004.

He Hao and Prabir Barooah are with the Department of Mechanical and Aerospace Engineering, University of Florida, Gainesville, FL 32611. Email: {hehao,pbarooah}@ufl.edu. Prashant G. Mehta is with the Coordinated Science Laboratory, Department of Mechanical Science and Engineering, University of Illinois, Urbana-Champaign, IL 61801. Email: mehtapg@uiuc.edu

Each vehicle i is allowed to use the following information in computing its control signal: (i) measurements of relative positions $p_i(t) - p_j(t)$, $j \in \mathcal{N}_i$, with respect to its neighbors as specified by the information graph, and (ii) its own velocity as well as the desired velocity of the formation. The control law is:

$$u_i^{(\mathrm{d})} = \sum_{j \in \mathcal{N}_i} -k_{(i,j)}^{(\mathrm{d})}(p_i^{(\mathrm{d})} - p_j^{(\mathrm{d})} - \Delta_{i,j}^{(\mathrm{d})}) - b_i^{(\mathrm{d})}(\dot{p}_i^{(\mathrm{d})} - v^{*(\mathrm{d})}),$$

where $i = 1, \ldots, N$, $v^{*(\mathrm{d})}$ is the d-th component of the desired velocity of the formation, $k_{(\cdot)}^{(\mathrm{d})}$ are proportional gains and $b_{(\cdot)}^{(\mathrm{d})}$ are derivative gains. The closed-loop dynamics of the i-th vehicle are obtained by combining the open loop dynamics (1) with the distributed control law, which yields

$$\ddot{p}_i = \sum_{j \in \mathcal{N}_i} -k_{(i,j)}(p_i - p_j - \Delta_{i,j}) - b_i(\dot{p}_i - v^*), \tag{2}$$

where the superscript d is suppressed since *the closed loop dynamics in each of the D_s spatial dimensions are decoupled* (due to the fully actuated assumption, and because the control input $u_i^{(\mathrm{d})}$ is based only on measurements taken along the d-th dimension).

Let $p_i^*(t)$ denote the desired trajectory of the i-th vehicle – this trajectory is uniquely determined by the trajectories of the reference vehicles and the desired formation geometry. For example, if r is a reference vehicle, then $p_i^*(t) = p_r^*(t) + \Delta_{i,r}^{(\mathrm{d})}$. To facilitate analysis, we define the following coordinate transformation: $\tilde{p}_i := p_i - p_i^*$, so that $\dot{\tilde{p}}_i = \dot{p}_i - v^*$. Substituting these into (2), we have

$$\ddot{\tilde{p}}_i = \sum_{j \in \mathcal{N}_i} -k_{(i,j)}(\tilde{p}_i - \tilde{p}_j) - b_i\dot{\tilde{p}}_i. \tag{3}$$

Since the trajectory of a reference vehicle is assumed to be equal to its desired trajectory, $\tilde{p}_r = 0$ if r is a reference vehicle. To express the closed-loop dynamics of the formation compactly, we define: $\psi := [\tilde{p}_1, \dot{\tilde{p}}_1, \ldots, \tilde{p}_N, \dot{\tilde{p}}_N]^T$. Using (3), the state-space model of the vehicle formation can now be written compactly as $\dot{\psi} = \mathbf{A}\psi$, where $\mathbf{A}$ is the closed-loop state matrix.

In this paper we restrict ourselves to lattices as information graphs:

Definition 2 (D-dimensional lattice): A D-dimensional lattice, specifically a $n_1 \times n_2 \times \cdots \times n_D$ lattice, is a graph with $n_1 n_2 \ldots n_D$ nodes. In the D-dimensional space $\mathbb{R}^D$, the coordinate of the i-th node is $\vec{i} := [i_1, \ldots, i_D]$, where $i_d \in \{0, 1, \ldots, (n_d - 1)\}$. An edge exists between two nodes $\vec{i}$ and $\vec{j}$ if and only if $\|\vec{i} - \vec{j}\| = 1$, where $\|\cdot\|$ is the Euclidean norm in $\mathbb{R}^D$. A $n_1 \times n_2 \times \cdots \times n_D$ lattice is denoted by $\mathbf{Z}_{n_1 \times n_2 \times \cdots \times n_D}$. □

A D-dimensional lattice is drawn in $\mathbb{R}^D$ with a Cartesian reference frame whose axes are denoted by $x_1, x_2, \ldots, x_D$.

Remark 1 (Spatial Dimension vs. Information Graph Dimension): The dimension D of the information graph is distinct from the spatial dimension D_s. Figure 1 depicts an example of two formations in space, one with $D_s = 1$ and the other with $D_s = 2$. The information graph, depicted in part (c) of the figure, is the same 3×3 two-dimensional lattice for either formation (i.e., $D = 2$). Note that the coordinate axes used in defining a lattice are, in general, not related to the coordinate axes in the physical space $\mathbb{R}^{D_s}$.

Due to the fully actuated nature of dynamics, the spatial dimension D_s plays no role in the results of this paper. The dimension of the information graph D, on the other hand, will be shown to play a crucial role. □

In this paper an information graph $\mathbf{G}$ is a lattice $\mathbf{Z}_{n_1 \times \cdots \times n_D}$, where $n_1 n_2 \ldots n_D = N + N_r$. For a given N, the choice of $N_r, D, n_1, n_2, \ldots, n_D$ determines the specific information graph within the class. An information graph is said to be *square* if $n_1 - 1 = n_2 = \ldots = n_D$.

For the ease of exposition, we only consider the following arrangement of lead (and therefore of the reference) vehicles:

Assumption 2: The reference vehicles are arranged so that a node $\vec{i} := [i_1, \ldots, i_D]$ in the information graph corresponds to a reference vehicle if and only if $i_1 = n_1 - 1$. □

Assumption 2 means that all reference vehicles are assumed to be arranged on a single "face" of the lattice, and every vehicle on this face is a reference vehicle. Therefore, $N = (n_1 - 1)n_2 \ldots n_D$ and $N_r = n_2 \ldots n_D$. Assumption 2 simplifies the presentation of the proposed methodology; other arrangements of reference vehicles can also be considered and some of these are described in [11].

III. PDE-BASED ANALYSIS AND DESIGN

Our goal is to analyze the closed-loop stability margin as function of the number of vehicles N and the information graph dimension D, and to devise ways to improve the stability margin by appropriately choosing the controller gains. Recall that the *stability margin* of the closed loop, denoted by S, is the absolute value of the real part of the least stable eigenvalue of the closed-loop state matrix. Instead of analyzing the state matrix, we proceed by first approximating the dynamics of the formation by a partial differential equation (PDE) model for large N. The PDE model yields insights that are useful for analysis and control design.

A. PDE model of the controlled vehicle formation

We first redraw the information graph in such a way so that it always lies in the unit D-cell $[0,1]^D$, irrespective of the number of vehicles. Note that in graph-theoretic terms, a graph is defined only in terms of its node and edge sets. A drawing of a graph in an Euclidean space, also called an embedding,is merely a convenient visualization tool. For the remainder of this section, we will consider the following drawing (embedding) of the lattice $\mathbf{Z}_{n_1 \times \cdots \times n_D}$ in the Euclidean space $\mathbb{R}^D$. The coordinate of the i-th node, whose "original" position was $[i_1, \ldots, i_D]$, is now drawn at position $[i_1 c_1, i_2 c_2, \ldots, i_D c_D]$, where $c_d := 1/(n_d - 1)$, for $d = 1, \ldots, D$.

The starting point of the PDE derivation is to consider a function $\tilde{p}(\vec{x}, t) : [0,1]^D \times [0, \infty) \to \mathbb{R}$ that satisfies: $\tilde{p}_i(t) = \tilde{p}(\vec{x}, t)|_{\vec{x}=[i_1 c_1, i_2 c_2, \ldots, i_D c_D]}$. A function that is originally defined at discrete points (the vertices of the lattice $\mathbf{Z}_{n_1 \times \cdots \times n_D}$) is approximated by a smooth function that is defined everywhere in $[0,1]^D$. The original function is obtained by sampling the smooth approximation.

For the i-th node with coordinate $\vec{i} = [i_1 c_1, \ldots, i_D c_D]$, we use i^{d+} and i^{d-} to denote the nodes with coordinates

$$i^{d+} := [i_1 c_1, \ldots, i_{d-1} c_{d-1}, (i_d + 1)c_d, i_{d+1} c_{d+1}, \ldots, i_D c_D],$$
$$i^{d-} := [i_1 c_1, \ldots, i_{d-1} c_{d-1}, (i_d - 1)c_d, i_{d+1} c_{d+1}, \ldots, i_D c_D],$$

respectively. The closed-loop dynamics (3) can now be expressed as:

$$\ddot{\tilde{p}}_i + b_i\dot{\tilde{p}}_i = -\sum_{d=1}^{D} k_{(i,i^{d+})}(\tilde{p}_i - \tilde{p}_{i^{d+}}) - \sum_{d=1}^{D} k_{(i,i^{d-})}(\tilde{p}_i - \tilde{p}_{i^{d-}}). \tag{4}$$

We next introduce the scalar functions $k_d^f, k_d^b, b : [0,1]^D \to \mathbb{R}$ (for $d \in \{1, \ldots, D\}$) defined according to the stipulation:

$$k_{(i,i^{d+})} = k_d^f(\vec{x})|_{\vec{x}=[i_1 c_1, \ldots, i_D c_D]}, \;\; k_{(i,i^{d-})} = k_d^b(\vec{x})|_{\vec{x}=[i_1 c_1, \ldots, i_D c_D]},$$
$$b_i = b(\vec{x})|_{\vec{x}=[i_1 c_1, \ldots, i_D c_D]}. \tag{5}$$

By using the following finite difference approximations for every $d \in \{1, \ldots, D\}$:

$$\left[\frac{\tilde{p}_{i^{d+}} - \tilde{p}_{i^{d-}}}{2c_d}\right] = \left[\frac{\partial \tilde{p}(\vec{x}, t)}{\partial x_d}\right]_{\vec{x}=[i_1 c_1, \ldots, i_D c_D]},$$
$$\left[\frac{\tilde{p}_{i^{d+}} - 2\tilde{p}_i + \tilde{p}_{i^{d-}}}{c_d^2}\right] = \left[\frac{\partial^2 \tilde{p}(\vec{x}, t)}{\partial {x_d}^2}\right]_{\vec{x}=[i_1 c_1, \ldots, i_D c_D]},$$

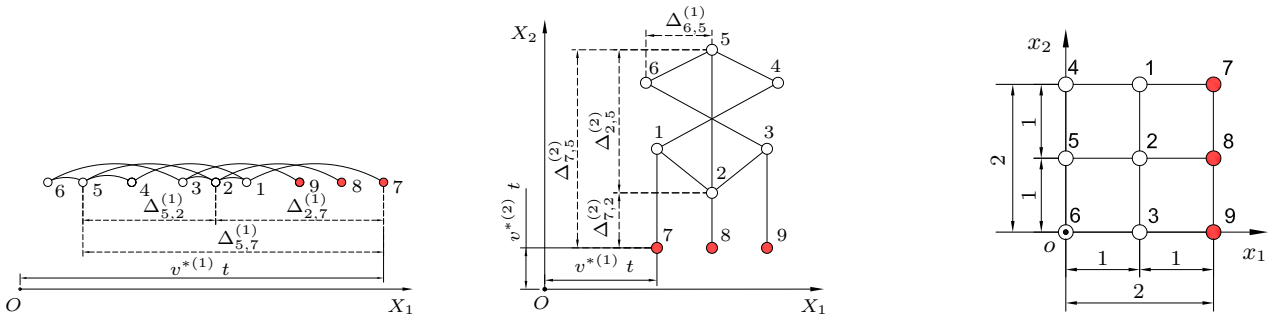

(a) A one-dimensional spatial formation. (b) A two-dimensional spatial formation. (c) The information graph for both (a) and (b).

Fig. 1. (a, b): Two distinct spatial formations that have the same associated information graph, which is shown in (c). Red (filled) circles represent fictitious reference vehicles and black (unfilled) circles represent real vehicles. Dashed lines (in (a), (b)) represent desired relative positions, while solid lines represent edges in the information graph.

the closed-loop dynamics (4) is seen as a finite difference approximation of the following PDE:

$$\Big(\frac{\partial^2}{\partial t^2}+b(\vec{x})\frac{\partial}{\partial t}\Big)\tilde{p}(\vec{x},t)=\sum_{d=1}^{D}\Big(\frac{k_d^f(\vec{x})-k_d^b(\vec{x})}{n_d-1}\frac{\partial}{\partial x_d}+\frac{k_d^f(\vec{x})+k_d^b(\vec{x})}{2(n_d-1)^2}\frac{\partial^2}{\partial {x_d}^2}\Big)\tilde{p}(\vec{x},t). \quad (6)$$

A more detailed derivation of (6) appears in [11], and is entirely analogous to the PDE derivation in [6] for the one-dimensional case. The PDE model (6) approximates the original coupled ODEs (3), and the approximation improves as each of the n_d's gets larger.

Under Assumption 2, the boundary condition of the PDE (6) is of the Dirichlet type on the face of the unit cell with the reference vehicles, and is of the Neumann type on all other faces:

$$\tilde{p}(1,x_2,\dots,x_D,t)=0,\ \frac{\partial\tilde{p}}{\partial x_1}(0,x_2,\dots,x_D,t)=0,$$
$$\frac{\partial\tilde{p}}{\partial x_d}(\vec{x},t)|_{x_d=0\text{ or }1}=0,\quad (d>1). \quad (7)$$

B. Stability margin with symmetric control

Definition 3: The control law is *symmetric* if every vehicle uses the same gains: $k_{(i,j)}=k_0$, for all $(i,j)\in\mathbf{E}$ and $b_i=b_0$ for all $i\in\mathbf{V}$, where k_0 and b_0 are positive constants. □

In case of symmetric control, we have for every $d=1,\dots,D$,

$$k_d^f(\vec{x})+k_d^b(\vec{x})=2k_0,\quad k_d^f(\vec{x})-k_d^b(\vec{x})=0,\quad b(\vec{x})=b_0,$$

and the PDE (6) simplifies to a damped wave equation:

$$\Big(\frac{\partial^2}{\partial t^2}+b_0\frac{\partial}{\partial t}\Big)\tilde{p}(\vec{x},t)=\mathcal{L}_0\tilde{p}(\vec{x},t), \quad (8)$$

where $\mathcal{L}_0$ is the Laplacian operator $\mathcal{L}_0=\sum_{d=1}^{D}\frac{k_0}{(n_d-1)^2}\frac{\partial^2}{\partial {x_d}^2}$. The analysis of the stability margin requires consideration of the eigenvalue problem

$$\mathcal{L}_0\phi(\vec{x})=-\lambda\phi(\vec{x}).$$

For the given boundary condition (7), the eigenvalues and eigenfunctions of $\mathcal{L}_0$ are given by

$$\lambda_{\vec{l}}=\pi^2k_0\Big(\frac{(2l_1-1)^2}{4(n_1-1)^2}+\frac{l_2^2}{(n_2-1)^2}+\cdots+\frac{l_D^2}{(n_D-1)^2}\Big),$$
$$\phi_{\vec{l}}=\cos\Big(\frac{(2l_1-1)\pi x_1}{2}\Big)\cos(l_2\pi x_2)\cdots\cos(l_D\pi x_D), \quad (9)$$

where $\vec{l}=(l_1,\dots,l_D)$ and $l_1\in\{1,2,\dots\}$, $l_2,\dots,l_D\in\{0,1,2,\dots\}$. The interested reader is referred to [12] for further discussion on the eigenvalues of PDEs.

The eigenvalues of the PDE are obtained in terms of $\lambda_{\vec{l}}$. Specifically, we consider a Fourier series expansion $\tilde{p}(\vec{x},t)=\sum\phi_{\vec{l}}(\vec{x})\alpha_{\vec{l}}(t)$. In these Fourier eigenfunction coordinates, taking a Laplace transform of (8) yields the characteristic equation $s^2+b_0s+\lambda_{\vec{l}}=0$. The two roots are $s_{\vec{l}}^{\pm}:=\frac{1}{2}\Big(-b_0\pm\sqrt{b_0^2-4\lambda_{\vec{l}}}\Big)$. If the discriminant $b_0^2-4\lambda_{\vec{l}}$ is positive, both the eigenvalues are real-valued. In this case, $s_{\vec{l}}^{+}$ is closer to the origin than $s_{\vec{l}}^{-}$; so we call $s_{\vec{l}}^{+}$ the $\vec{l}$-th *less-stable* eigenvalue. The *least stable* eigenvalue is the one among these that is closest to the imaginary axis, and the stability margin is the absolute value of its real part. The least stable eigenvalue can be obtained by minimizing $\lambda_{\vec{l}}$ over the D-tuple $(l_1,\dots,l_D)$. Using (9), we see that this minimum is achieved at $l_1=1,l_2=\cdots=l_D=0$, where $\lambda_{(1,0,\dots,0)}=\frac{\pi^2k_0}{4(n_1-1)^2}$. Therefore,

$$s_{\min}:=\min_{(l_1,\dots,l_D)}s_{\vec{l}}^{+}=\frac{b_0}{2}\Big(-1+\Big(1-\frac{\pi^2k_0}{b_0^2(n_1-1)^2}\Big)^{1/2}\Big)$$
$$=-\frac{\pi^2k_0}{4b_0(n_1-1)^2}+O(\frac{1}{n_1^4}),$$

where the last equality holds when $n_1\gg 1+\pi\sqrt{k_0}/b_0$. The stability margin is $S=|Re(s_{\min})|$, and the analysis above leads to the following result for the stability margin.

Theorem 1: Consider a vehicle formation with closed-loop dynamics (3). With symmetric control under Assumption 2, the stability margin S of the PDE model (8) of the closed loop dynamics has the asymptotic formula

$$S=\frac{\pi^2k_0}{4b_0}\frac{1}{(n_1-1)^2}+O(\frac{1}{n_1^4}), \quad (10)$$

that holds as $n_1\to\infty$. □

This result tells us that the stability margin of the vehicle formation depends only upon n_1 – the number of vehicles along the x_1 axis. The x_1 axis is special because it is normal to the face of the graph with the reference vehicles. In the PDE model, the boundary condition is of the Dirichlet type on this face (see (7)). Analogous estimates also hold with different arrangement of the reference vehicles (see [7], [11] for details).

1) Square information graph: For a square information graph, $N=(n_1-1)n_2\dots n_D=(n_1-1)^D$, and it follows from Theorem 1 that the stability margin is given by

$$S=\frac{\pi^2k_0}{4b_0}\frac{1}{N^{2/D}}+O(\frac{1}{N^{4/D}}). \quad (11)$$

This shows that for a constant choice of symmetric control gains k_0 and b_0, the stability margin approaches 0 as $N\to\infty$. The dimension D of the information graph determines the exponent of

the scaling law for S. For example, the stability margin scales as $O(1/N^2)$ for a one-dimensional information graph and as $O(1/N)$ for a two-dimensional information graph. Thus, *for the same control gains, increasing the dimension of the information graph improves the stability margin significantly*. In practice, this may require long range communication, since neighbors in the information graph need not be physically close. Recall that an information graph is a drawing of the connectivity.

2) Non-square information graph: Consider a *non-square* information graph with $n_1 = O(N^c)$, where $c \in [0,1]$ is a fixed constant. From Theorem 1, it follows that $S = O(1/N^{2c})$. By choosing $c < 1/D$, the loss of stability margin S as a function of N can be slowed down, as compared to the square lattice. Thus, within the class of D-dimensional lattices and fixed N, certain information graphs provide better scaling of the stability margin than others. In fact, by holding n_1 to be a constant independent of the number of vehicles N, the stability margin can be bounded away from zero even as the number of vehicles increases without bound. The price one pays for such improvement is the increased number of lead vehicles. This is the case because $N_r = N/(n_1 - 1)$ by Assumption 2.

It is important to stress that not all non-square graphs are advantageous. For example, if $n_1 = O(N)$ and n_2 through n_D are $O(1)$, it follows from Theorem 1 that the stability margin S is $O(1/N^2)$. This is the same asymptotic trend as in a one-dimensional information graph. In this case, the D dimensional information graph effectively behaves as a one-dimensional graph.

Figure 2 provides numerical corroboration of the results. The stability margin S as a function of N for three distinct two-dimensional information graphs are shown. The margin obtained by computing the eigenvalues of the closed-loop state matrix $\mathbf{A}$ is compared against the prediction by Theorem 1. The plots show Theorem 1 provides an excellent prediction of the stability margin trends.

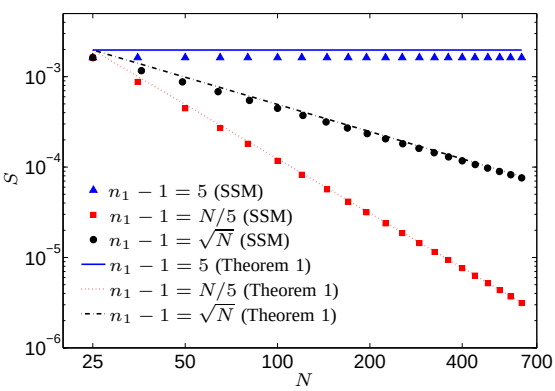

Fig. 2. Stability margin predicted by Theorem 1 for a vehicle formation with two-dimensional information graphs of different "aspect ratios". The control gains used are $k_0 = 0.01$, $b_0 = 0.5$. The legend "SSM" (abbreviation of "state-space model") means the stability margin is determined from numerical computation of eigenvalues of the state matrix $\mathbf{A}$. For the first case, $n_1 - 1 = 5$ and $n_2 = N/5$. Theorem 1 predicts that in this case $S = O(1)$. In the second case, $n_2 = 5$ and $n_1 - 1 = N/5$, which leads to $S = O(1/N^2)$. The third case is that of a square information graph, $n_1 - 1 = n_2 = \sqrt{N}$, for which $S = O(1/N)$.

C. Mistuning-based (asymmetric) control design

We next consider the effect of small perturbation to the nominally symmetric control. The objective of the *mistuning*-based control design is to introduce such perturbations with the goal of improving the scaling law for the stability margin.

Specifically, we consider gain profiles $k_d^f(\vec{x}) = k_0 + \varepsilon \tilde{k}_d^f(\vec{x})$, $k_d^b(\vec{x}) = k_0 + \varepsilon \tilde{k}_d^b(\vec{x})$, where $\varepsilon > 0$ is a small parameter signifying the small amount of mistuning and $\tilde{k}_d^f(\vec{x})$, $\tilde{k}_d^b(\vec{x})$ are *mistuning profiles* that satisfy $\|\tilde{k}_d^f(\vec{x})\|_\infty = 1$ and $\|\tilde{k}_d^b(\vec{x})\|_\infty = 1$. That is, for every d, we require $\sup_{\vec{x}} |k_d^f(\vec{x}) - k_0| \leq \varepsilon$ and $\sup_{\vec{x}} |k_d^b(\vec{x}) - k_0| \leq \varepsilon$. Define $\tilde{k}_d^s(\vec{x}) := \tilde{k}_d^f(\vec{x}) + \tilde{k}_d^b(\vec{x})$ and $\tilde{k}_d^m(\vec{x}) := \tilde{k}_d^f(\vec{x}) - \tilde{k}_d^b(\vec{x})$. The PDE (6) now becomes

$$\Big(\frac{\partial^2}{\partial t^2} + b_0 \frac{\partial}{\partial t}\Big)\tilde{p}(\vec{x},t) = \sum_{d=1}^{D} \Big(\frac{k_0}{(n_d-1)^2}\frac{\partial^2}{\partial x_d^2}\Big)\tilde{p}(\vec{x},t) + \varepsilon \sum_{d=1}^{D} \Big(\frac{\tilde{k}_d^s(\vec{x})}{2(n_d-1)^2}\frac{\partial^2}{\partial x_d^2} + \frac{\tilde{k}_d^m(\vec{x})}{n_d-1}\frac{\partial}{\partial x_d}\Big)\tilde{p}(\vec{x},t). \quad (12)$$

The control problem is to design the functions $\tilde{k}_d^s(\vec{x})$ and $\tilde{k}_d^m(\vec{x})$ to maximize the stability margin. For small mistuning, the solution to this problem is given by the following theorem:

Theorem 2: Consider the problem of maximizing the stability margin of PDE (12) by designing the proportional control gains $k_d^{(\cdot)}$, where the gains are required to satisfy $|k_d^{(\cdot)} - k_0| \leq \varepsilon$, with $\varepsilon > 0$ being a small pre-specified constant. The optimal control gains are given by:

$$k_1^f(\vec{x}) = k_0 + \varepsilon,\ k_1^b(\vec{x}) = k_0 - \varepsilon,\ k_d^{(\cdot)}(\vec{x}) = k_0\ (d \geq 2). \quad (13)$$

The resulting stability margin is given by

$$S = \frac{2\varepsilon}{b_0}\frac{1}{n_1 - 1} + O(\frac{1}{n_1^2}). \quad (14)$$

The formula is asymptotic in the sense that it holds when $n_1, \ldots, n_D \to \infty$ and $\varepsilon \to 0$. □

It follows from the result above that the corresponding optimal control gains for the i-th vehicle ($i = 1, 2, \ldots, N$) are $k_{(i,i^{1+})} = k_0 + \varepsilon, k_{(i,i^{1-})} = k_0 - \varepsilon$ and $k_{(i,j)} = k_0$ for all other neighbors j. That is, the nominally symmetric control gains are mistuned *only* along the x_1 axis (normal to the face with reference vehicles).

Comparing Theorems 1 and 2, we see that the effect of mistuning is to introduce a square root in the stability margin formula. For the special case of a square information graph, the stability margin is given by $S = \frac{2\varepsilon}{b_0}\frac{1}{N^{1/D}} + O(\frac{1}{N^{2/D}})$. Thus, even for small values of ε, mistuning can improve the closed-loop stability margin by a significant amount, especially when the number of vehicles is large. Note that the improvement over symmetric control is brought about by changes in the proportional gains $k_i^{(\cdot)}$ alone. Changes in the derivative gains b_i do not affect the asymptotic trend of the stability margin. Using the same perturbation method as in the proof of Theorem 2, we can see that it is not possible to reduce it to $O(1/n_1)$ ($O(1/N^{1/D})$ for square information graph) by small changes in the derivative gains.

Numerical verification appears in Figure 3. The proportional control gains are perturbed from their nominal symmetric values by $\pm 10\%$. The figure shows that i) the eigenvalues of the PDE (12) closely match the closed-loop eigenvalues of the formation ($\mathbf{A}$ matrix), and ii) the mistuned eigenvalues show significant improvement compared to the nominally symmetric case. The improvement is particularly noticeable for large values of N, while being significant even for small values of N.

Proof of Theorem 2. [sketch, see [11] for details] The proof proceeds by using a perturbation method. The eigenvalues are obtained by taking the Laplace transform of the perturbed PDE (12). For $\varepsilon = 0$, the eigenvalues $s_{\vec{l}}^{(0)}$ and the corresponding eigenfunction $\phi_{\vec{l}}^{(0)}$ have already been obtained (see (9)). Denoting $\mathcal{P}(s) := s^2 + b_0 s - \mathcal{L}_0$,

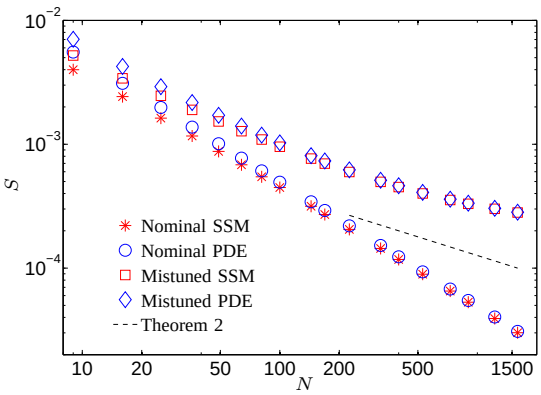

Fig. 3. Improvement in the stability margin S by mistuning for a vehicle formation with two-dimensional square information graph. The nominal control gains are $k_0 = 0.01$, $b_0 = 0.5$, and the mistuning amount is $\pm 10\%$ ($\varepsilon = 0.001$). The legends "SSM" and "PDE" correspond to the state-space model and the PDE model, respectively, while "nominal" corresponds to symmetric control.

we have $\mathcal{P}(s_{\vec{l}}^{(0)})\phi_{\vec{l}}^{(0)} = 0$. For $\varepsilon > 0$, we consider the eigensolution in terms of regular perturbation about the $\varepsilon = 0$ solution:

$$s_{\vec{l}} = s_{\vec{l}}^{(0)} + \varepsilon s_{\vec{l}}^{(\varepsilon)} + O(\varepsilon^2), \quad \phi_{\vec{l}} = \phi_{\vec{l}}^{(0)} + \varepsilon \phi_{\vec{l}}^{(\varepsilon)} + O(\varepsilon^2).$$

The $O(\varepsilon)$ balance gives:

$$\mathcal{P}(s_{\vec{l}}^{(0)})\phi_{\vec{l}}^{(\varepsilon)} = \Big(\sum_{d=1}^{D} \frac{k_d^m(\vec{x})}{n_d - 1} \frac{\partial}{\partial x_d} + \sum_{d=1}^{D} \frac{k_d^s(\vec{x})}{2(n_d-1)^2} \frac{\partial^2}{\partial x_d^2} - b_0 s^{(\varepsilon)} - 2 s_{\vec{l}}^{(0)} s_{\vec{l}}^{(\varepsilon)} \Big) \phi_{\vec{l}}^{(0)} =: R.$$

For a solution $\phi_{\vec{l}}^{(\varepsilon)}$ to exist, R must lie in the range space of the operator $\mathcal{P}(s_{\vec{l}}^{(0)})$. Since $\mathcal{P}(s_{\vec{l}}^{(0)})$ is self-adjoint, the range space is orthogonal to its null space. So, $< R, \phi_{\vec{l}}^{(0)} >= 0$. We thus have the following equation:

$$\int_0^1 .. \int_0^1 \Big(\sum_{d=1}^{D} \frac{k_d^m(\vec{x})}{n_d - 1} \frac{\partial \phi_{\vec{l}}^{(0)}}{\partial x_d} + \sum_{d=1}^{D} \frac{k_d^s(\vec{x})}{2(n_d-1)^2} \frac{\partial^2 \phi_{\vec{l}}^{(0)}}{\partial x_d^2} - b_0 s_{\vec{l}}^{(\varepsilon)} \phi_{\vec{l}}^{(0)} - 2 s_{\vec{l}}^{(0)} s_{\vec{l}}^{(\varepsilon)} \phi_{\vec{l}}^{(0)} \Big) \phi_{\vec{l}}^{(0)} dx_1..dx_D = 0.$$

Setting $l_1 = 1$ and $l_d = 0$ for $d > 1$ and following straightforward manipulations, we obtain an asymptotic formula for the least stable eigenvalue of PDE (12),

$$s_{\min} = s_{\min}^{(0)} - \frac{\varepsilon \pi}{2 b_0 (n_1 - 1)} \int_0^1 \tilde{k}_1^m(\vec{x}) \sin\left(\pi x_1\right) \, dx_1 - \frac{\varepsilon \pi^2}{4 b_0 (n_1 - 1)^2} \int_0^1 \tilde{k}_1^s(\vec{x}) \cos^2(\frac{\pi}{2} x_1) \, dx_1 + O(\varepsilon^2),$$

where $s_{\min}^{(0)}$ is the least stable eigenvalue for the $\varepsilon = 0$ problem. To minimize the real part of the least stable eigenvalue, we need to only choose $\tilde{k}_1^m(\vec{x})$, because the term involving $\tilde{k}_1^m(\vec{x})$ is of order $1/(n_1 - 1)$, whereas the term involving $\tilde{k}_1^s(\vec{x})$ is of order $1/(n_1-1)^2$. Therefore, we set

$$\tilde{k}_d^s(\vec{x}) \equiv 0 \equiv \tilde{k}_d^m(\vec{x}) \quad \text{for} \quad d = 2, \ldots, D, \text{ and } \tilde{k}_1^s(\vec{x}) \equiv 0.$$

This leads to $\tilde{k}_1^f(\vec{x}) = -\tilde{k}_1^b(\vec{x}) \Leftrightarrow \tilde{k}_1^m(\vec{x}) = 2\tilde{k}_1^f(\vec{x})$. The stability margin is maximized by making the integral $\int_0^1 \tilde{k}_1^m(\vec{x}) \sin(\pi x_1) dx_1$ as large as possible. To do so, we set $\tilde{k}_1^m(\vec{x})$ to be the largest possible value everywhere in the unit cell subject to the constraint $|k_d^{(\cdot)} - k_0| \leq \varepsilon$. This give us the optimal control gains given in (13), and the stability margin formula also follows. ■

D. Approximation error

The PDE model (6) is an approximation of the coupled-ODE model (3) of the formation. Our analysis of the stability margin of the formation (Theorem 1) is based on the least stable eigenvalue of the PDE. The mistuning-based control design is also arrived at by designing for the PDE. For the conclusions derived from the PDE-based analysis to be valid, one must address the following question: is the least stable eigenvalue obtained from the PDE model a good approximation of the least stable eigenvalue of the ODE model? The answer happens to be yes, as the following result shows.

Lemma 1: With symmetric control (respectively, mistuning control specified in Theorem 2), the difference between the stability margin of the PDE model (6)-(7) and of the coupled-ODE model (3) is $O(1/n_1^3)$ (respectively, $O(1/n_1^2) + O(\varepsilon^2)$). □

We see from the result above that the ratio of the difference between the stability margin predictions by the PDE and ODE models to the stability margin itself is $O(1/n_1)$, which is small for large n_1. The proof of the result is not included here due to space constraints; the interested reader is referred to [11, Lemma 1].

IV. Time domain simulation

We now present results of the time-domain simulations that provide further corroboration of the results, that the stability margin can be improved by (i) using a higher-dimensional information graph with symmetric control; and ii) by using mistuned control gains for the same information graph. For the first set of simulations, we consider $N = 25$ vehicles in a one-dimensional formation ($D_s = 1$). The initial position and velocity of each vehicle are randomly drawn from a uniform distribution on $[-0.01, 0.01]$. We carry out simulations with two distinct information graphs for the same physical formation: a 26 nodes (including 1 reference vehicle) one-dimensional lattice and 6×5 nodes (including 5 reference vehicles) two-dimensional lattice. Figures 4 (a) and (b) depict the trajectories of the position errors of the vehicles, for the one-dimensional and two-dimensional information graphs, respectively. In both cases, the control law is symmetric with gains $k_0 = 0.01$, $b_0 = 0.5$. Comparing Figure 4 (a) and (b), we see that the transients due to initial conditions decay faster with the two-dimensional information graph compared to the one-dimensional case. This improvement is consistent with the result of Theorem 1. The second set of simulations are carried out to verify the effect of mistuning. We consider a formation with 15×15 vehicles and 15 reference vehicles employing a square two-dimensional information graph – a 16×15 nodes two-dimensional lattice. The initial position and velocity of each vehicle are again chosen as random small perturbation of the desired position and velocity. Figures 5 (a) and (b) depict the trajectories of the position errors with symmetric and mistuned control gains, respectively. For the symmetric case, the control gains are $k_0 = 0.01$, $b_0 = 0.5$. For the mistuned case $\varepsilon = 0.001$, i.e., the gains $k_{(i,j)}$ are perturbed by $\pm 10\%$ from the nominal symmetric value k_0. Comparing Figure 5 (a) and (b), we see that the transients due to initial conditions decay faster for the mistuned design as compared to the symmetric case. This improvement is consistent with results of Theorem 2.

V. Discussion

We studied the closed-loop stability margin with distributed control of a network of N vehicles, each modeled using a double integrator. The effect of two main factors on the stability margin was examined: (i) the structure of the information graph (within the class of D dimensional lattices), and (ii) asymmetry in the use of information from neighboring vehicles.

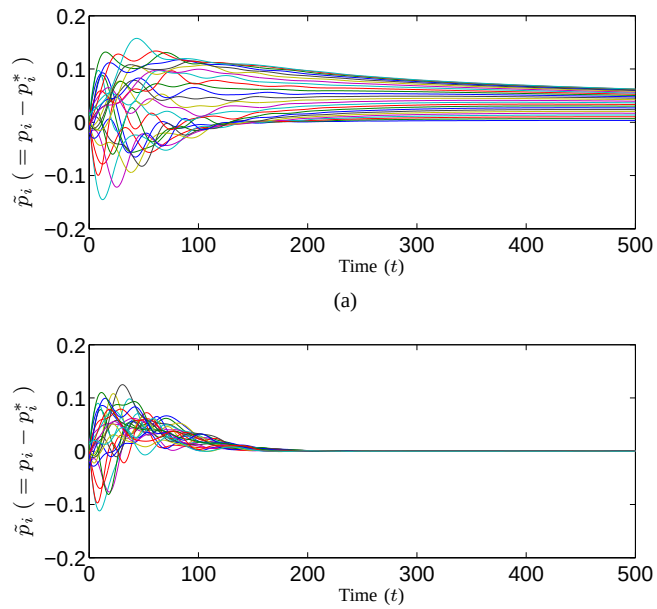

(a)

(b)

Fig. 4. Comparison of symmetric control's performance for the same formation with one-dimensional and two-dimensional information graphs respectively.

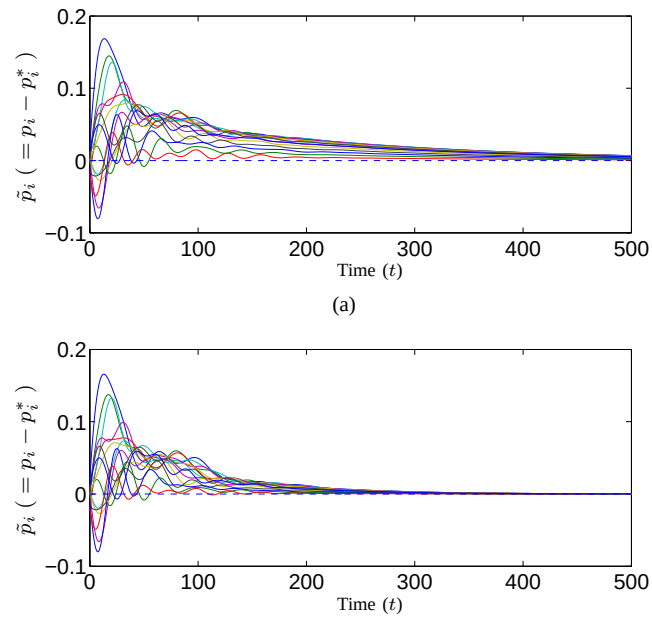

(a)

(b)

Fig. 5. Comparison of time-domain performance between symmetric and mistuned control with the same 16×15 nodes (including 15 reference vehicles) two-dimensional square information graph. Only the first 15 vehicles' errors are shown.

For a square lattice with symmetric control, the stability margin approaches zero as $O(1/N^{2/D})$ as $N \to \infty$. Therefore, the stability margin can be improved by increasing the dimension of the information graph. For a non-square information graph, the stability margin can be made nearly independent of the number of vehicles by choosing the "aspect ratio" appropriately. The trade-off is that increasing the dimension of the information graph or choosing a beneficial aspect ratio may require long range communication and/or entail an increase in the number of lead vehicles. Our results are therefore useful in investigating design trade-offs between performance and the cost of designing information architectures for distributed control.

The other main contribution of this paper is the mistuning-based control design. We showed that the stability margin can be improved significantly by using a small amount of asymmetry (mistuning) in control gains. In particular, for square lattices the stability margin can be improved to $O(1/N^{1/D})$, which is significant, especially for large N. The additional information needed to implement the mistuned control (as compared to the symmetric control) is minimal: every vehicle should know the mistuning parameter ε and the indices of its neighbors in the information graph.

The results of the paper are derived by analysis of a PDE approximation of the coupled-ODE model of the formation dynamics. The PDE model provides insight into the role of asymmetry that the coupled ODE model does not.

Although this paper considered only the arrangement of reference vehicles on one face of the graph; it is straightforward to extend the analysis to more general boundary conditions. In terms of exponent of the scaling law, the asymptotic trend of the stability margin with N does not change with different arrangements of the boundary conditions (additional details appear in [7], [11]).

References

[1] H.-S. Tan, R. Rajamani, and W.-B. Zhang, "Demonstration of an automated highway platoon system," in *American Control Conference*, vol. 3, June 1998, pp. 1823 – 1827.

[2] P. M. Ludwig, "Formation control for multi-vehicle robotic minesweeping," Master's thesis, Naval postgraduate school, 2000.

[3] A. J. Fax and R. M. Murray, "Information flow and cooperative control of vehicle formations," *IEEE Transactions on Automatic Control*, vol. 49, pp. 1465–1476, September 2004.

[4] P. Barooah and J. P. Hespanha, "Graph effective resistances and distributed control: Spectral properties and applications," in *Proc. of the 45th IEEE Conference on Decision and Control*, December 2006, pp. 3479–3485.

[5] B. Bamieh, M. R. Jovanović, P. Mitra, and S. Patterson, "Effect of topological dimension on rigidity of vehicle formations: fundamental limitations of local feedback," in *Proceedings of the 47th IEEE Conference on Decision and Control*, Cancun, Mexico, 2008, pp. 369–374.

[6] P. Barooah, P. G. Mehta, and J. P. Hespanha, "Mistuning-based decentralized control of vehicular platoons for improved closed loop stability," *IEEE Transactions on Automatic Control*, vol. 54, no. 9, pp. 2100–2113, September 2009.

[7] H. Hao, P. Barooah, and P. G. Mehta, "Distributed control of two dimensional vehicular formations: stability margin improvement by mistuning," in *ASME Dynamic Systems and Control Conference*, October 2009.

[8] G. Lionis and K. Kyriakopoulos, "Decentralized lattice formation control for micro robotic swarms," in *IEEE/RSJ International Conference on Intelligent Robots and Systems (IROS)*, October 2009, pp. 3756 –3761.

[9] A. Sarlette and R. Sepulchre, "A PDE viewpoint on basic properties of coordination algorithms with symmetries," in *48th IEEE Conference on Decision and Control*, December 2009, pp. 5139–5144.

[10] G. Ferrari-Trecate, A. Buffa, and M. Gati, "Analysis of coordination in multi-agent systems through partial difference equations," *IEEE Transactions on Automatic Control*, vol. 51, no. 6, pp. 1058 – 1063, 2006.

[11] H. Hao, P. Barooah, and P. G. Mehta, "Stability margin scaling laws for distributed formation control as a function of network structure," *ArXiV.org*, May 2010. [Online]. Available: http://arxiv.org/abs/1005.0351

[12] L. Evans, *Partial Differential Equations: Second Edition (Graduate Studies in Mathematics)*. American Mathematical Society, 2010.